AJNR

Multiplanar metrizamide-enhanced CT imaging of the foramen magnum.

D L LaMasters, T J Watanabe, E F Chambers, D Norman and T H Newton

This information is current as of August 11, 2025.

Multiplanar Metrizamide-Enhanced CT Imaging of the Foramen Magnum

David L. LaMasters[1]
Ted J. Watanabe[2]
Evan F. Chambers[3]
David Norman[3]
Thomas H. Newton[3]

Definition of masses and malformations at the foramen magnum has been less than optimal with traditional radiographic techniques. The use of intrathecal metrizamide with computed tomographic (CT) scanning improves contrast resolution and facilitates detection of abnormalities that may not be apparent on Pantopaque cisternography, plain films, or conventional axial CT alone. Fifty patients with clinically suspected foramen-magnum lesions were evaluated with this technique. Forty were abnormal with the following findings: 14 cases of the Chiari malformation (five cases had associated syringomyelia), five meningiomas, three neuromas, a chondrosarcoma, a chordoma, and five cervical and three brainstem gliomas. Six cases of syringomyelia, a large posterior-fossa subarachnoid cyst, and an anomaly of the cisterna magna were also diagnosed. Sagittal and coronal images were beneficial in defining tonsillar position, configuration of the fourth ventricle, and the relations of mass lesions to the spinal canal and subarachnoid space. Metrizamide CT cisternography provides superior spatial and contrast resolution of lesions at the foramen magnum not obtainable with other radiographic techniques. Morbidity is minimal because of the low dose of metrizamide used. Multiplanar reformations are particularly helpful in assessing anatomic detail not readily recognized on axial scans alone.

Evaluation of lesions at the craniovertebral junction is difficult, both clinically and radiographically. The "missed" foramen magnum tumor, in particular, has received significant emphasis in the medical literature [1, 2]. The delay in diagnosis of abnormalities in this location often arises because of a nonspecific or unusual clinical presentation [3]. However, even if the diagnosis of a lesion at the foramen magnum is suspected, it may be missed if the myelographic or computed tomographic (CT) evaluation is inadequate [4, 5].

Metrizamide CT cisternography improves the diagnostic accuracy and simplifies the radiographic workup of pathology at the foramen magnum. When this procedure is combined with CT reformation, the nature, extent, and definition of masses or congenital abnormalities at the craniovertebral junction may be analyzed in more detail. We believe that multiplanar reconstruction with metrizamide CT cisternography obviates myelography in this region.

Subjects and Methods

Fifty consecutive patients with symptoms referable to the foramen magnum region were studied using the technique of combined CT scanning and metrizamide cisternography. Symptoms in this group included suboccipital headaches, dysesthesias of the upper extremities, gait disturbance, dizziness, and astereognosis. Physical findings included upper and lower extremity weakness, hemiparesis, tetraparesis, spasticity, and ataxia. Although plain films, tomography, angiography, and conventional axial CT had been performed in many instances, these were often nondiagnostic or inconclusive.

Metrizamide CT cisternography was performed either as a primary CT study or as an adjunct to metrizamide myelography. In the primary metrizamide CT study, 4–5 ml of 170

TABLE 1: **Clinical Entities at Foramen Magnum**

Abnormal Findings	No.
Extraaxial masses:	
Meningioma	5
Neurinoma (C2 and cranial nerve XII)	3
Chondrosarcoma	1
Chordoma	1
Intraaxial masses:	
Cervical glioma	5
Brainstem glioma	3
Congenital malformations:	
Chiari I*	8
Chiari II	6
Syringomyelia†:	
Traumatic syrinx	1
Syringomyelia	5
Miscellaneous:	
Subarachnoid cyst	1
Anomalous cisterna magna	1
Total	40

* One case of Chiari I was associated with Klippel-Feil and basilar invagination.

† Five additional cases of syrinx were detected in association with the Chiari malformations.

mg/ml I metrizamide was injected into the lumbar subarachnoid space using a 22 gauge spinal needle. The patient was then titled 45° head-down in the prone position for 3 min to facilitate diffusion of the contrast agent into the upper cervical subarachnoid space and cisterns of the posterior fossa.

When metrizamide CT cisternography is performed after myelography, the CT scans are obtained about 4–6 hr after the primary myelographic study. This delay prevents untoward side effects. The concentration of the contrast agent at 4–6 hr remains high enough to allow an adequate examination of this region.

All 50 patients were scanned on a G.E. 8800 CT/T scanner with at 120 kVp, 320 mA, and a scan speed of 9.6 sec. Axial scans were obtained in a plane parallel to the infraorbitomeatal line. Collimation of 5 mm with a table motion of 3 mm increments (2 mm overlap) was used. The patients were scanned from the level of the fourth ventricle to the upper cervical region, usually to the level of C2, resulting in about 20–25 axial scans. If an enlarged brainstem or cervical cord had been detected on the initial axial scans, the patient was rescanned about 4 hr later in an attempt to demonstrate filling of a central cavity.

After completion of the axial scan, reformatted images were generated using the GEDIS (General Electric Medical Systems Division) 6.21 software package. The planes to be reformatted depended on the particular clinical problem. Using the GEDIS software package, up to four axial images may be displayed simultaneously to select the appropriate planes for subsequent sagittal, coronal, paraaxial, or oblique reformations. A trackball cursor system was used to designate the appropriate reformation plane on the axial image. The software protocol then generates a specified plane from the stored axial data.

Results

Of the 50 patients studied using the technique of metrizamide CT cisternography, 40 were abnormal (table 1). The lesions were divided into extraaxial masses, intramedullary tumors, syringomyelia-syringobulbia, and congenital malformations.

Satisfactory reformatted images were obtained in 46 of the 50 patients. The rest were degraded by patient motion during and between axial scans, teeth fillings producing registration artifacts, and residual Pantopaque from prior myelograms or cisternograms. Reformations were assessed in each case to determine the size of the foramen magnum, the contour of the cord and brainstem, the position of the cerebellar tonsils, and the presence of mass or congenital lesions.

Normal Anatomy: Reformatted Images

The anatomy of the craniovertebral junction on axial CT cisternograms has been described by several authors [6–9]. Multiplanar reformations are less familiar and will be briefly discussed.

Midline structures such as the upper cervical cord, medulla oblongata, fourth ventricle, and cerebellar vermis are best assessed on a median sagittal reformation (fig. 1A). The clivus in its relation to the atlas and axis is apparent. The fourth ventricle is identified between the pons and the vermis. The position of the fourth ventricle may be assessed from the midsagittal reformatted image using the method of Twining (fig. 1B) [10]. In the 10 normal studies, the midpoint of Twining's line was found to lie at or slightly anterior to the floor of the fourth ventricle. This differs minimally from pneumoencephalographic measurements, where the midpoint of Twining's line falls at or posterior to the floor of the fourth ventricle. That position is most likely positional, as pneumoencephalography requires assessment of the fourth ventricle with the patient semiprone while in CT cisternography the patient is supine.

Parasagittal images are used to determine the position of the cerebellar tonsils (fig. 2). This particular reformation was most beneficial in assessing the Chiari type I malformation and the degree of tonsillar herniation. The vertebral arteries may be seen in the parasagittal plane as they pass around the lateral aspect of the medulla.

The axis of the brainstem is obliquely oriented to the orbitomeatal plane (usually at 75°). An oblique coronal image generated from a sagittal reformation permits a second view of the entire neural axis from the upper cervical cord through the cerebral peduncles (fig. 3). The neural axis is narrowest at the cervicomedullary junction. It abruptly widens at the level of the pons where the middle cerebellar peduncles diverge laterally into the cerebellar hemispheres.

Coronal reformations perpendicular to the orbitomeatal plane were used with the parasagittal reformations to assess the shape and position of the cerebellar tonsils (fig. 4). The tonsils normally have a rounded contour and appear as discrete structures posterior to and separate from the lower medulla. While the tonsils may reach the level of the foramen magnum, extension below the outer table is abnormal [11].

The axis of the foramen magnum often does not lie in the orbitomeatal plane. A tangential paraaxial reformation overcomes this difficulty and allows the foramen magnum to be seen in its entirety (fig. 5). The foramen magnum is ellipsoid, measuring about 3.2–3.6 cm anteroposteriorly and 2.5–3.4 cm from side to side [12].
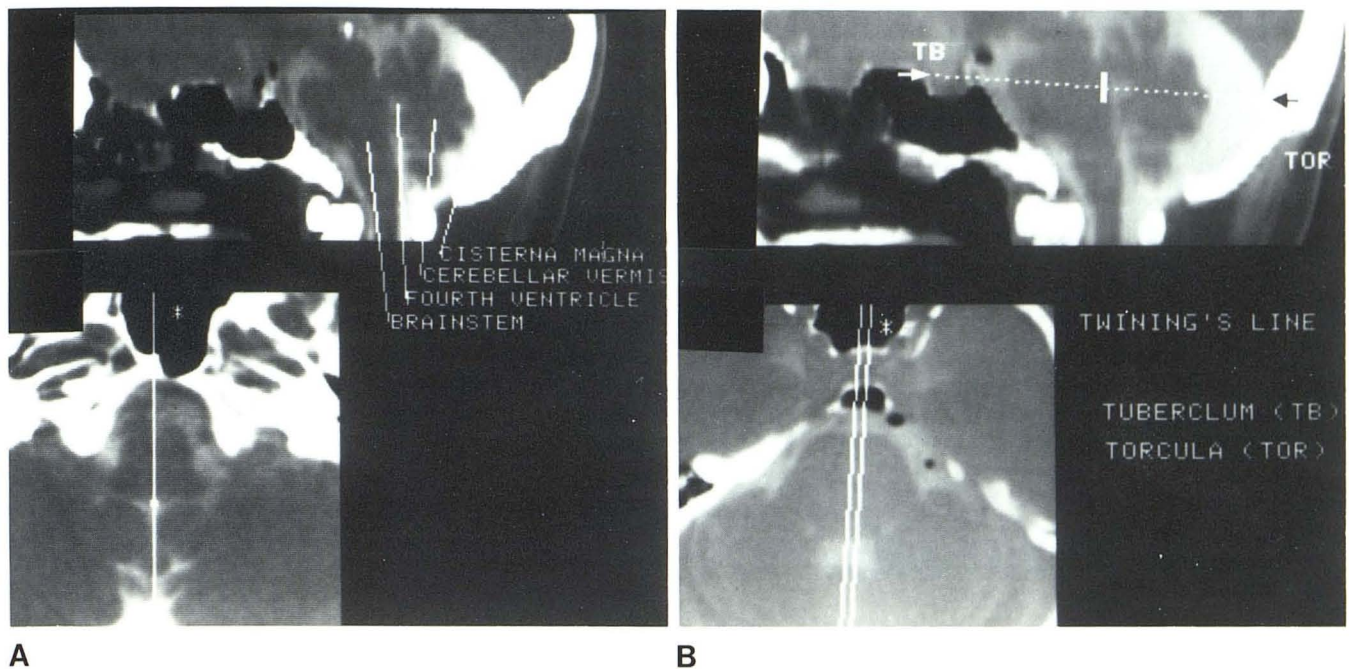
A

B

Fig. 1.—A, Midline sagittal reformation. Neural axis and cerebellar vermis defined. B, Position of fourth ventricle may be assessed by method of Twining, using midline sagittal reformation. With metrizamide CT cisternog-

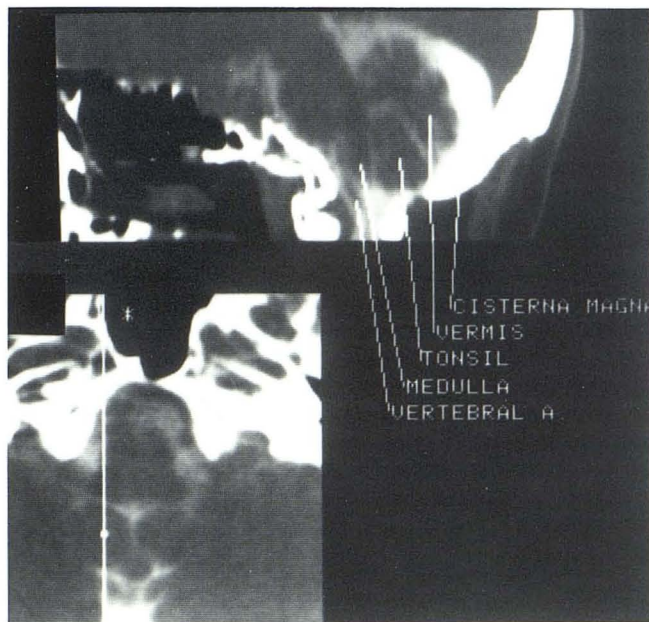raphy, midpoint of Twining's line lies at or slightly anterior to floor of fourth ventricle (*vertical white bar*).

Fig. 2.—Parasagittal reformation. Cerebellar tonsil outlined by metrizamide.

Representative Case Reports

Case 1

A 76-year-old woman had burning dysesthesias in her left hand. Physical examination demonstrated mild left upper and lower extremity weakness and diminished sensation to pin-prick and vibra-

tion. Cerebrospinal fluid (CSF) protein was 400 mg/dl. Initial Pantopaque myelography was nondiagnostic, as the injection was partially subdural. Intravenous-contrast-enhanced CT of the foramen magnum was normal (fig. 6A). Metrizamide CT cisternography demonstrated a mass at the craniocervical junction (fig. 6B). Reformatted images clearly showed a cleavage plane between the mass and the upper cervical cord (figs. 6C and 6D). The lesion was excised totally and proved to be an extradural meningioma arising at the level of the foramen magnum.

Case 2

A 13-year-old boy had a 7 month history of weakness in the left arm and hand. Physical examination revealed decreased motor strength in both upper extremities, greater on the left. Pain sensation was diminished in the hands. Widening of the cervical cord was noted at myelography (fig. 7A). Metrizamide CT cisternography demonstrated enlargement of the entire cervical cord with extension to the foramen magnum (fig. 7B). A small cystic cavity filled with contrast material at C3 (fig. 7D). A midline sagittal reformation showed the full extent of the mass (fig. 7C). At biopsy, the lesion proved to be an ependymoma of the cervical cord.

Case 3

A 15-year-old boy with known Klippel-Feil syndrome developed paresthesias of the right arm and hand associated with weakness of grip about 7 weeks before admission. Metrizamide myelography demonstrated a widened cervical cord from C2 to C7. Delayed metrizamide CT cisternography showed filling of a syrinx, tonsillar ectopia, occipitalization of C1, and basilar invagination. The diagnosis of Chiari type I with associated syringomyelia was established (fig. 8).
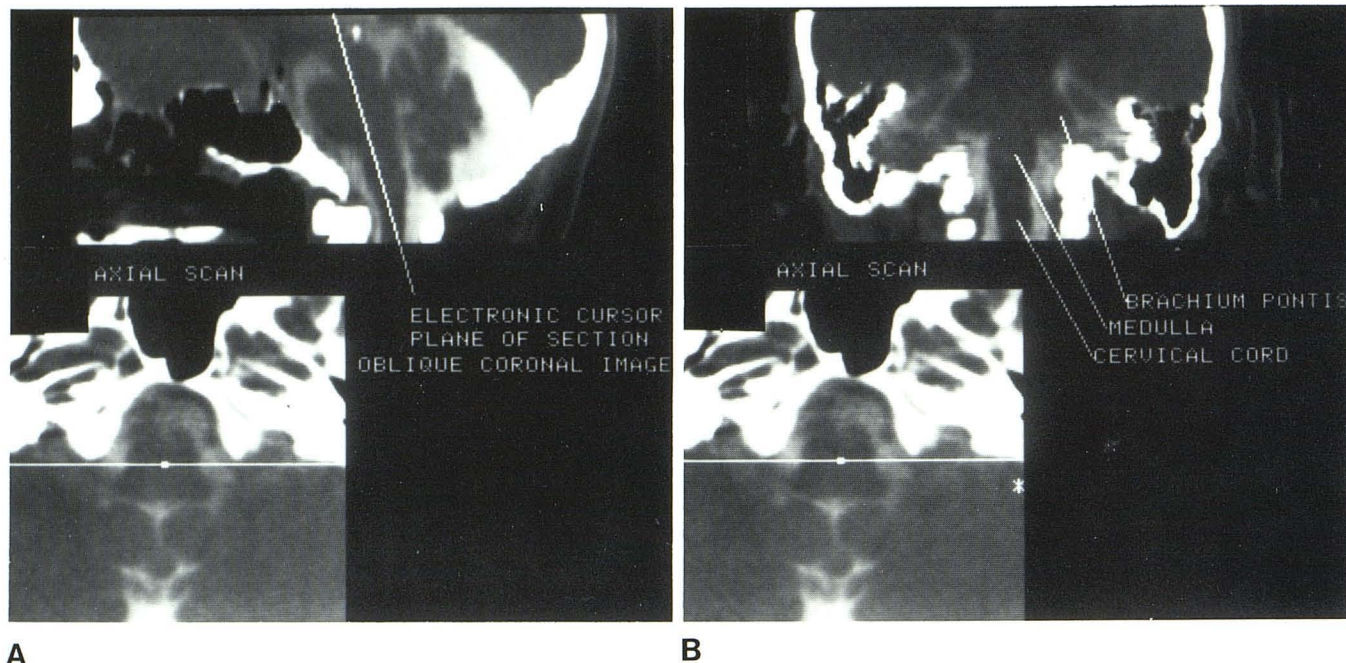
A

B

Fig. 3.—**A**, Midsagittal section with cursor specifies plane of section for oblique coronal reformation. **B**, Oblique coronal demonstrates cerebellar peduncles, medulla, pons, mesencephalon, and cerebellar hemispheres.
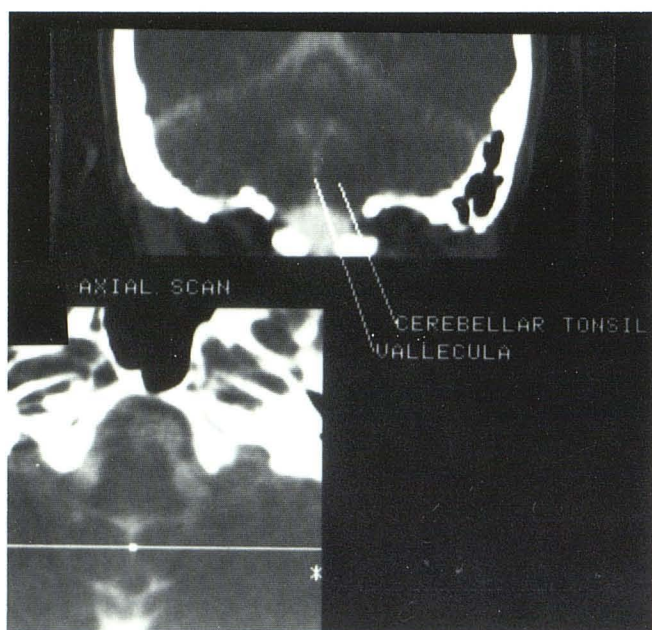

Fig. 4.—Coronal reformation. Tonsil position is above outer table of foramen magnum.

Case 4

A 58-year-old man had a clivus chordoma subtotally resected and subsequently treated with radiation therapy. Three years later he developed severe occipital headaches. CT demonstrated recurrence of the tumor in the sphenoid, sella, and petrous regions (fig.

9A). The conventional CT study suggested that the brainstem may have been invaded by the chordoma. Metrizamide CT cisternography was performed to assess the integrity of the dura and exclude invasion of the brainstem. A sagittal section showed the large extraaxial clival mass deflecting the dura posteriorly without evidence of frank invasion of the brainstem (fig. 9B).

Case 5

A 13-year-old girl developed imbalance. Conventional CT demonstrated an enhancing pontine mass, probably representing a brainstem glioma. The tumor was treated with chemotherapy and 5,440 rad (54.4 Gy) to the posterior fossa. Follow-up CT scan 6 months later suggested that the lesion was larger, although the patient's clinical examination was stable (fig. 10A). Metrizamide CT cisternography demonstrated that the mass extended into the right pyramid and inferior cerebellar peduncle. Although the enlargement of the brainstem continued to the level of the foramen magnum, it did not extend beyond the limits of the previous radiation port (figs. 10B–10D).

Case 6

A 60-year-old woman had a 2 year history of increasing numbness in both hands, more noticeable on the right. A carpal-tunnel release procedure produced little improvement. Recently, she noted decreased grip strength in both hands. Physical findings on admission included slight gait ataxia and diminished grip strength on the ulnar side of the right hand. Cervical myelography demonstrated subtle effacement of the right aspect of the cervical subarachnoid space at C1 (fig. 11A). Follow-up metrizamide CT cisternography clearly demonstrated an extradural mass at C1–C2 adjacent to the right C2 neural foramen (figs. 11B and 11C). At surgery, a nerve sheath tumor of the C2 root was excised.
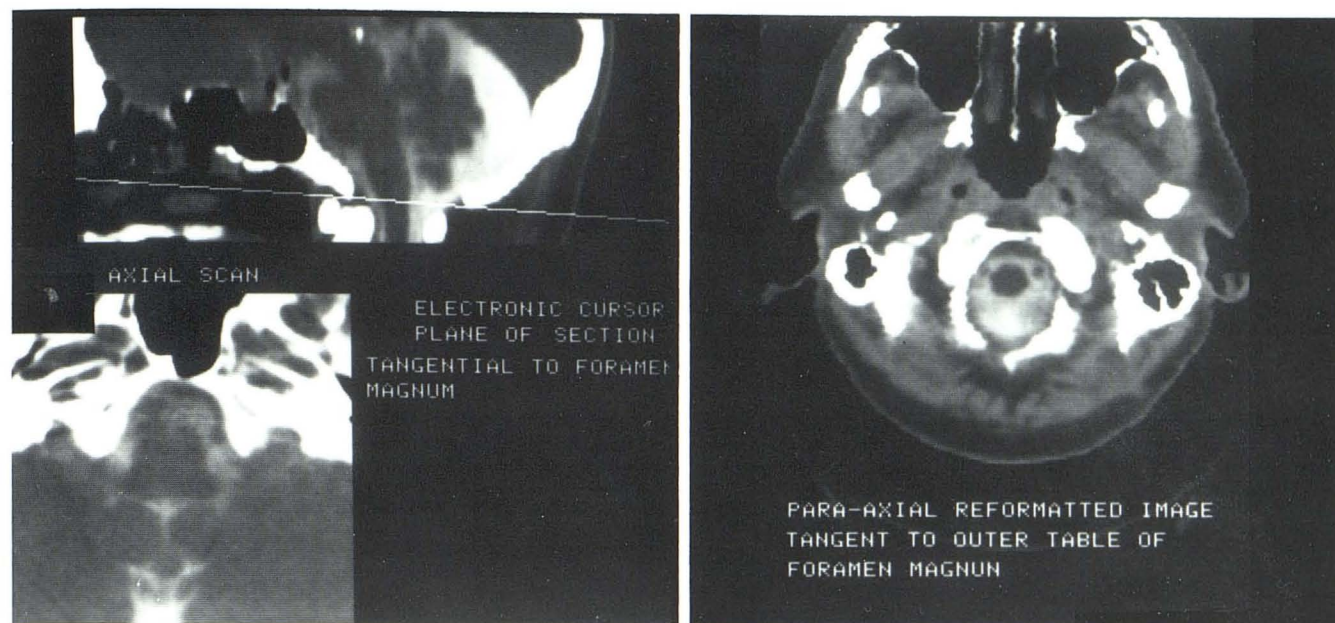
A

B

Fig. 5.—**A**, Sagittal section with paraaxial reformation defined by cursor. **B**, Tangential section through foramen magnum demonstrates its normal size and contour.
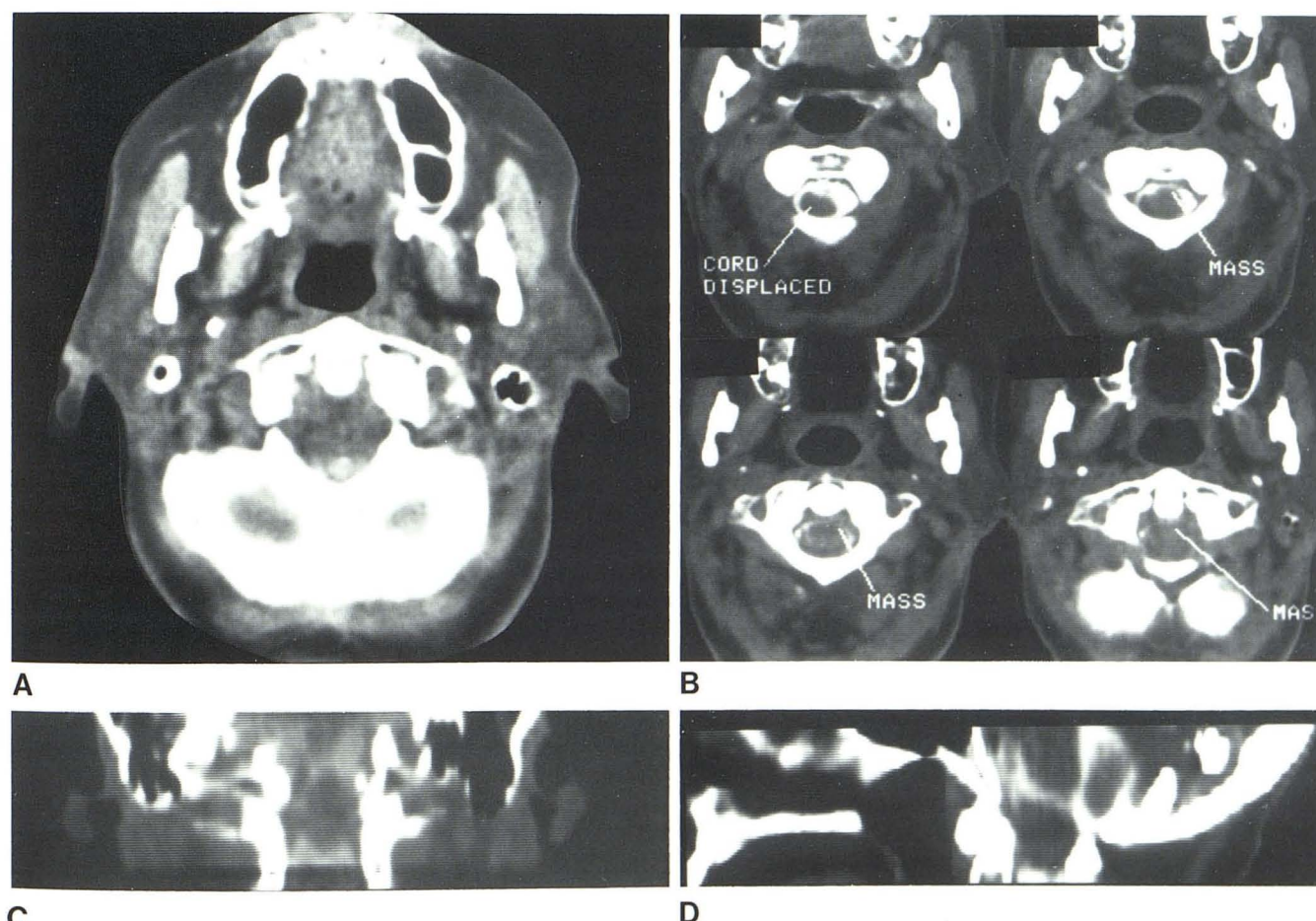

A

B

C

D

Fig. 6.—Meningioma at foramen magnum. **A**, Unremarkable initial conventional CT. **B**, Axial sections with metrizamide show mass and deviation of cord. **C** and **D**, Reformatted images clearly define lesion as separate from cervical cord.

A

B

ENLARGED
CERVICAL
CORD

C

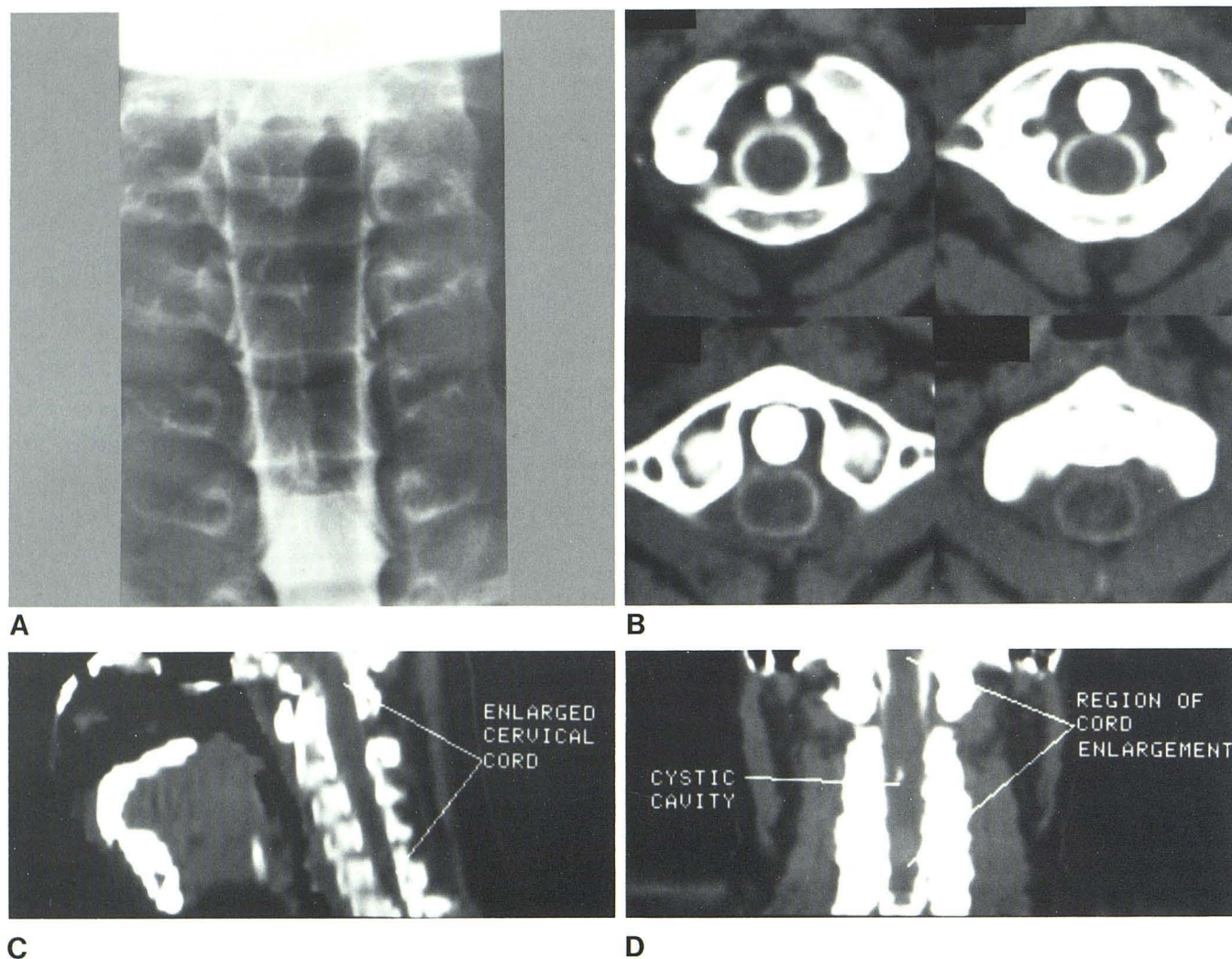CYSTIC
CAVITY

REGION OF
CORD
ENLARGEMENT

D

Fig. 7.—Ependymoma of cervical cord extending into lower medulla. **A,** Metrizamide myelogram. Fusiform widening of cervical spinal cord. Axial CT images (**B**) and midsagittal reformation (**C**) show cephalad extent of tumor to foramen magnum. **D,** Coronal section defines small metrizamide-filled cystic cavity.

Discussion

Diagnosis of lesions at the craniovertebral junction poses a significant dilemma for the clinical neurologist and neurosurgeon, as well as the neuroradiologist. Both mass lesions and congenital abnormalities, such as the Chiari type I malformation, may be symptomatic many years before accurate diagnosis [13]. Symptoms are often not specific for a foramen magnum process, and early clinical signs may be entirely attributed to cervical spondylosis or misdiagnosed as multiple sclerosis [1, 3, 14, 15].

Although the clinical diagnosis of a foramen magnum process is admittedly difficult, when early physical findings and symptoms are identified, the radiologist must undertake a complete evaluation of this region. Various radiologic imaging methods have been used to study the craniovertebral junction, including Pantopaque cisternography, verte-

bral angiography, pneumoencephalography, and plain radiography. Little mention, however, is found in the literature concerning the utility of computed tomography in evaluating the craniovertebral junction.

Pantopaque cisternography has for many years been the method of choice in assessing possible lesions near the foramen magnum [16–18]. Both prone and supine examinations are required to depict the upper cervical subarachnoid space and cisterns of the posterior fossa. Although this technique displays the structures in and around the foramen magnum well, it requires considerable operator expertise. Permanent deposition of Pantopaque in the posterior fossa cisterns is undesirable because this agent creates significant registration artifacts on CT scans, limiting the effectiveness of CT as a follow-up method. Many investigators do not include supine cisternography as an adjunct to cervical Pantopaque myelography to exclude a dorsally placed for-
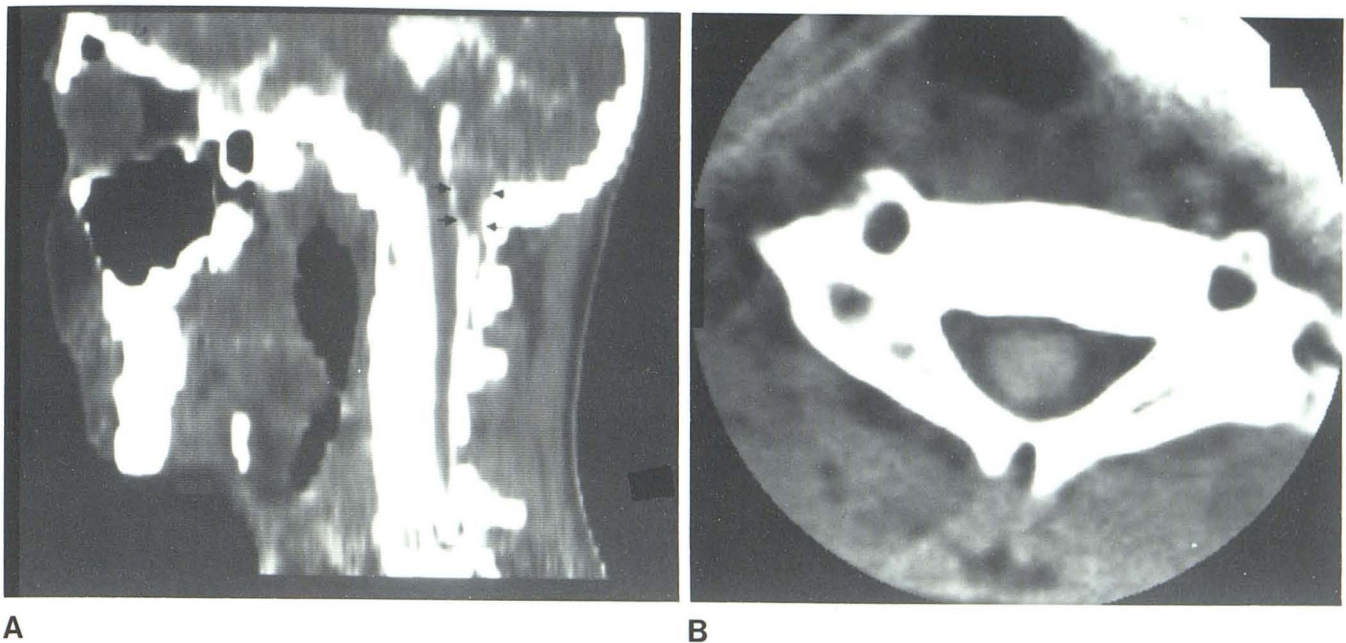
Fig. 8.—Chiari I with syringomyelia. **A,** Parasagittal reformation. Tonsillar ectopia. **B,** Syrinx cavity documented on delayed scan.
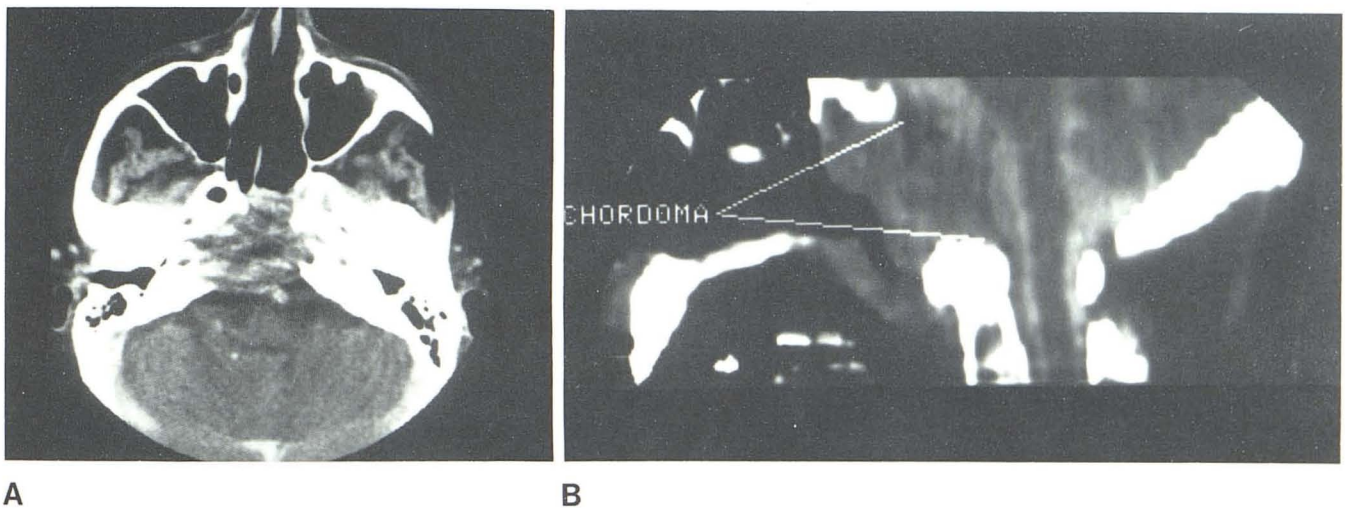

Fig. 9.—Clivus chordoma. **A,** Conventional CT. Marked destruction of clivus and sphenoid and suggestion of direct invasion of brainstem. **B,** Midline sagittal metrizamide study. Neural axis is intact.

amen magnum lesion in patients with a nonspecific clinical presentation.

Plain film metrizamide cisternography of the craniovertebral junction can be performed, but adverse reactions (nausea, vomiting, seizures) make this approach undesirable [19]. With cervical myelography, the dorsal aspect of the foramen magnum region is usually not depicted, in an effort to avoid spilling high-concentration (220–250 mg/ml I) metrizamide into the basal cisterns. Although delayed CT ex

amination of the foramen magnum after myelography has been suggested by Skalpe and Sortland [20], there are few reports to indicate that this has been widely adopted.

Computed tomography without intrathecal enhancement is inadequate in evaluating most lesions at the foramen magnum. Several of the representative cases shown exemplify the difficulty of relying on conventional CT alone to define extraaxial masses or the extent of intraaxial lesions beyond the level of the foramen magnum. Although Spallone
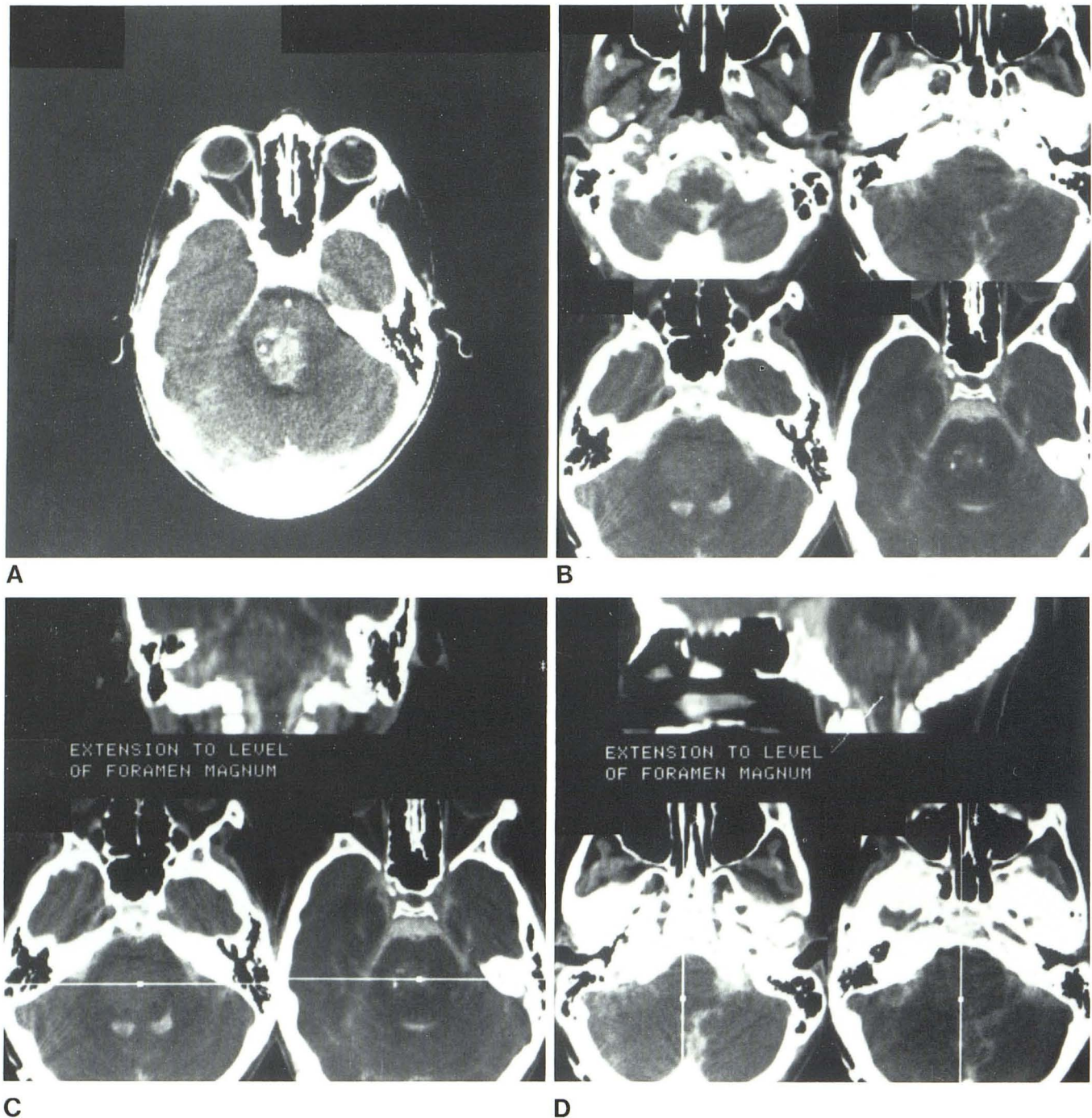
Fig. 10.—Brainstem glioma. **A**, Conventional CT. Glioma centered at pons. **B**, Metrizamide CT cisternogram shows caudal extent to foramen magnum and better estimates overall magnitude of tumor (**C** and **D**).

et al. [21] reported two patients with tumors defined by CT without metrizamide, both lesions were large and one had associated bony changes noted on plain film. The inherently poor contrast resolution and concurrent inability to routinely define intraspinal contents with current CT scanners limited the usefulness of CT without intrathecal enhancement [22].

The efficacy of metrizamide CT cisternography has been documented in the evaluation of other central nervous system mass lesions. Recent reports describe the use of metrizamide CT cisternography in evaluating the brainstem [23, 24], in differentiating partially empty sella from intrasellar tumor [25], and in assessing the spinal canal, particularly in the diagnosis of syringomyelia [26, 27]. In a series of 75 patients with a suspected syrinx, the central cavity was
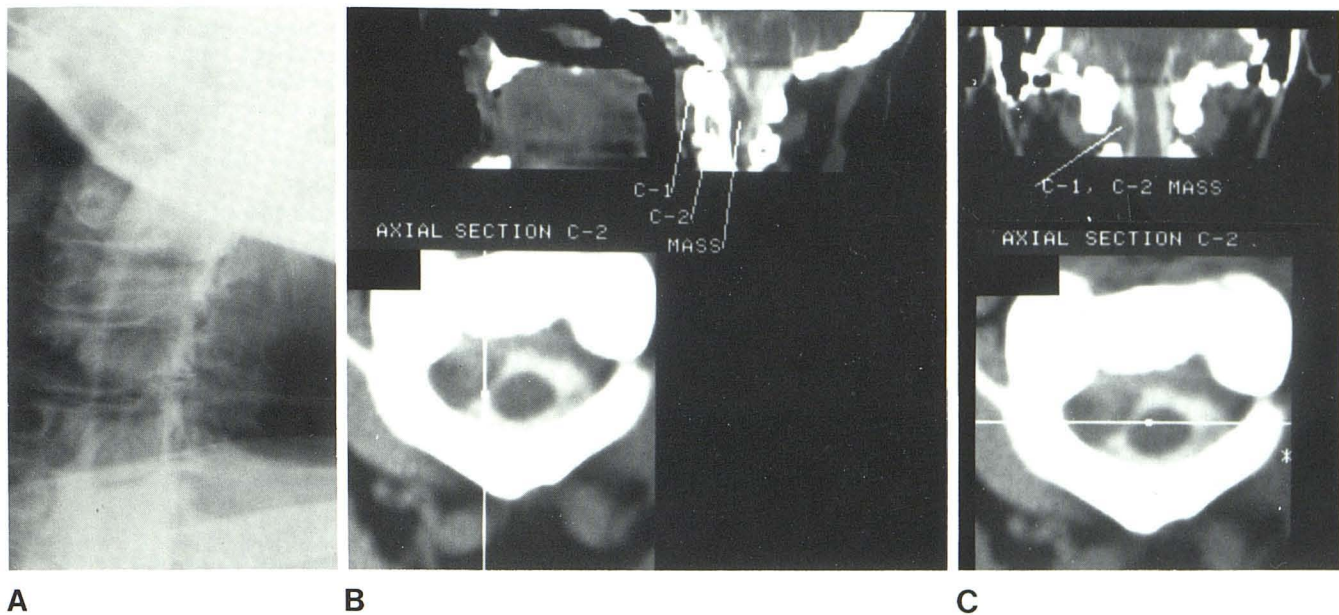
A **B** **C**

Fig. 11.—Schwannoma C1–C2. **A**, Myelogram. Subtle effacement of subarachnoid space at C1–C2. **B**, Parasagittal reformation. Mass is better appreciated. **C**, Coronal section best demonstrates relation of tumor to neural foramen.

successfully demonstrated in 67 [28]. The routine use of metrizamide CT cisternography in the radiologic diagnosis of foramen magnum lesions, however, has not been emphasized.

Our experience with metrizamide CT cisternography suggests that it is a sensitive technique in the diagnosis of craniovertebral pathology. The use of intrathecal metrizamide improves contrast resolution, allowing identification of structures not routinely seen on conventional CT studies. The upper cervical cord, medulla, inferior vermis, lower cranial nerves, vertebral and basilar arteries, posterior fossa cisterns, and fourth ventricles are routinely imaged with this technique. Minor effacements of the cisterns and subtle changes in the contour of the neural axis are more apparent than with conventional computed tomography (cases 1, 4–6).

Reformatted images have proven most useful in demonstrating the spatial relations of a mass lesion to the neural axis and the osseous canal. In instances where axial sections may show apparent continuity of a mass with the cord, reformatted images may allow definition of a cleavage plane confirming the extraaxial nature of the lesion (case 1). Displacement of the cord by extraaxial mass is perceived with little difficulty on sagittal and oblique coronal reformations.

In the Chiari malformation, the position of the tonsils and the contour of the medullary cervical junction are best appreciated in sagittal and parasagittal planes. Because of the high incidence of associated syrinx, metrizamide CT cisternography is also ideal for evaluating a coexisting central cavity. Similarly, the degree of cerebellar tonsillar ectopia is best appreciated on sagittal and coronal reformatted views. The structure may then be visualized on a single image as opposed to a series of axial sections.

The superior anatomic resolution provided by metrizamide CT cisternography should render Pantopaque cisternography obsolete in the evaluation of foramen magnum pathology. The combined use of image reformations further facilitates recognition of spatial relations at the craniovertebral junction. Untoward side effects are uncommon due to the low doses of metrizamide used. In patients with clinical manifestations of a foramen magnum lesion, we recommend metrizamide CT cisternography as the initial radiographic examination.

REFERENCES

1. Howe JR, Taren JA. Foramen magnum tumors. Pitfalls in diagnosis. *JAMA* **1973**;225:1061–1066
2. Missed foramen magnum tumors (editorial). *Lancet* **1973**; 2:1482
3. Cohen L, MacRae D. Tumors in the region of the foramen magnum. *J Neurosurg* **1962**;19:462–469
4. Aring CD. Lesions about the junction of medulla and spinal cord. *JAMA* **1974**;229:1879
5. Bull J. Missed foramen magnum tumors. *Lancet* **1974**;1:91
6. Drayer BP, Rosenbaum AE, Higman HB. Cerebrospinal fluid imaging using serial metrizamide CT cisternography. *Neuroradiology* **1977**;13:7–17
7. Rosenbaum AE, Drayer BP. CT cisternography with metrizamide. *Acta Radiol [Suppl]* (Stockh) **1977**;355:323–337
8. Drayer BP, Rosenbaum AE. Studies of the third circulation. *J Neurosurg* **1978**;48:946–956
9. Drayer BP, Rosenbaum AE, Rergel DB, Bank WO, Deeb ZL. Metrizamide CT cisternography: pediatric applications. *Radiology* **1977**;124:349–357
10. Hilal SK, Tookoran H, Wood BS. Displacement of the aqueduct of Sylvius by posterior fossa tumors. *Acta Radiol [Diagn]* (Stockh) **1969**;9:167–182
11. Wickbom I, Hanafee W. Soft tissue masses immediately below

the foramen magnum. *Acta Radiol* **1963**;1:647–658

12. Coin CG, Malkasian DR. Foramen magnum. In: Newton TH, Potts, DG, eds. *Radiology of the skull and brain*, vol. 1. St. Louis: Mosby, **1971**:275–286

13. Marc JA, Schechter MM. Radiological diagnosis of mass lesions within and adjacent to the foramen magnum. *Radiology* **1975**;114:351–365

14. Symonds CP, Meadows SP. Compression of the spinal cord on the neighborhood of the foramen magnum. *Brain* **1937**;60:52–84

15. Abbott RH. Foramen magnum and high cervical cord lesions simulating degenerative disease of the nervous system. *Ohio State Med J* **1950**;46:645–651

16. Baker H. Myelographic examination of the posterior fossa with positive contrast medium. *Radiology* **1963**;81:791–801

17. Malis LI. Myelographic examination of the foramen magnum. *Radiology* **1958**;70:196–221

18. Mones R, Werman R. Pantopaque myeloencephalography. *Radiology* **1959**;72:803–809

19. Wylie IG, Afshar F, Koege TH. Results of the use of a new water soluble contrast medium (metrizamide) in the posterior fossa of the baboon. *Br J Radiol* **1975**;48:1007–1010

20. Skalpe IO, Sortland O. Cervical myelography with metrizamide (Amipaque). *Neuroradiology* **1978**;16:275–278

21. Spallone A, Tanfani G, Vissilouthis J, Dazzi N. Benign extramedullary foramen magnum tumors diagnosis by computed tomography. *J Comput Assist Tomogr* **1980**;4:225–229

22. Davis KR, Taveras JM, Roberson GH, Ackerman RH. Some limitations of computed tomography in the diagnosis of neurological diseases. *AJR* **1976**;127:111–123

23. Steele JR, Hoffman JC. Brainstem evaluation with CT cisternography. *AJNR* **1980**;1:521–526

24. Glanz S, Geehr RB, Duncan CC, Piepmeier JM. Metrizamide-enhanced CT for evaluation of brainstem tumors. *AJNR* **1980**;1:31–34

25. Gross CE, Binet ET, Esquerra JV. Metrizamide cisternography in the evaluation of pituitary adenomas and the empty sella. *J Neurosurg* **1979**;50:472–476

26. Bonafe A, Ethier R, Melancon D, Belanzer G, Peters T. High resolution computed tomography in cervical syringomyelia. *J Comput Assist Tomogr* **1980**;4:142–147

27. DiChiro G, Axelbaum SP, Schillinger D, et al. Computerized axial tomography in syringomyelia. *N Engl J Med* **1975**; 292:13–16

28. Aubin ML, Vignaud J, Jardin C, Bar D. Computed tomography in 75 clinical cases of syringomyelia. *AJNR* **1981**;2:199–204